Hindawi Publishing Corporation
International Journal of Antennas and Propagation
Volume 2015, Article ID 102959, 8 pages
http://dx.doi.org/10.1155/2015/102959

Research Article

A Multibeam Dual-Band Orthogonal Linearly Polarized Antenna Array for Satellite Communication on the Move

Yi Liu,[1] Hu Yang,[1] Shaojun Mao,[2] and Jiang Zhu[1]

[1]*College of Electronic Science and Engineering, National University of Defense Technology, Changsha 410073, China*
[2]*Southwest Electronics and Telecommunication Technology Research Institute, Chengdu, Sichuan 610041, China*

Correspondence should be addressed to Yi Liu; yi_liu@nudt.edu.cn

Received 24 July 2015; Accepted 8 October 2015

Academic Editor: Ernest Okon

The design and simulation of a 10 × 8 multibeam dual-band orthogonal linearly polarized antenna array operating at Ku-band are presented for transmit-receive applications. By using patches with different coupling methods as elements, both perpendicular polarization in 12.25–12.75 GHz band and horizontal polarization in 14.0–14.5 GHz band are realized in a shared antenna aperture. A microstrip Rotman lens is employed as the beamforming network with 7 input ports, which can generate a corresponding number of beams to cover −30°–30° with 5 dB beamwidth along one dimension. This type of multibeam orthogonal linearly polarized planar antenna is a good candidate for satellite communication (SatCom).

1. Introduction

The ever increasing need for ubiquitous satellite communication (SatCom) services on the move in land, maritime, and aeronautical environments pushes the development of mobile antenna systems. The known mobile antenna systems can be generally divided into three types by scanning styles. The first type utilizes fully mechanical steering system like a traditional reflector array or a multibeam lens antenna [1, 2]. The second type uses RF topologies like the classical phased array approach or Digital Beam Forming (DBF) which are completely electronically steerable [3]. The third type merges the technologies of mechanical steering and electronic steering together for planar antennas [4, 5]. The main disadvantages of mechanical steering systems are that the resulting user terminals are not low profile, heavy and/or bulky, subject to G-forces, and maintenance intensive [6]. With naturally low profile, the primary barrier for phased array antennas to gain a larger share of the market is the expensive cost. These properties of the previous two types are limitations to commercial exploitation in the automotive, maritime, and airborne applications in the civil field. But the emerging technology of beamforming network, like Rotman lens [7], provides a solution to implement a one-dimension electronically steerable antenna instead of costly phase shifters. Combining mechanical steering technology in another dimension, the mobile antenna system is capable of providing near-hemispherical coverage. Far more attractive are hybrid mechanically/electronically steerable solutions, which can be low profile and simultaneously possess fast and accurate pointing capabilities.

Providing high data rate satellite communications is of important significance to deliver mission-critical data, voice, and video, for secure and real-time information flow. Among the operating frequencies of mobile antennas, Ku-band is being viewed increasingly as its advantages of low cost and wide bandwidth in broadcasting services and bidirectional links which can compete with terrestrial networks [6]. For a satellite communications system with simultaneous transmit-receive operation, the center frequencies of receiving and transmitting should be different with orthogonal polarization values. The orthogonal linearly polarized antennas have been employed in many broadcasting and communicating satellites.

To achieve more benefits according to the previous analysis, in this paper, a dual band orthogonal linearly

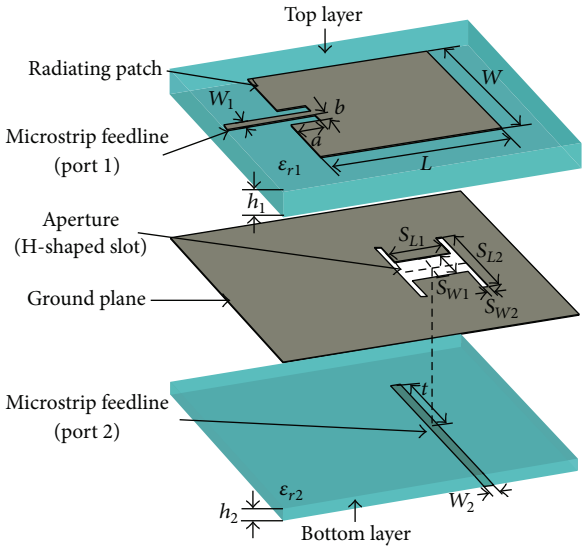

Figure 1: Geometry of a dual-polarized rectangular patch antenna fed by coplanar microstrip line feed and slot-coupled feed.

Table 1: Parameter of the antenna element.

Parameter	Description	Value
W	Width of radiating patch	6.40 mm
L	Length of radiating patch	6.10 mm
a	Length of matching slot	0.99 mm
b	Width of matching slot	0.45 mm
h_1	Thickness of top layer	0.93 mm
h_2	Thickness of bottom layer	0.43 mm
S_{W1}	Width of H-shaped slot's center arm	1.53 mm
S_{L1}	Length of H-shaped slot's center arm	1.89 mm
S_{W2}	Width of H-shaped slot's side arm	0.20 mm
S_{L2}	Length of H-shaped slot's side arm	4.01 mm
W_1	Width of top feedline	0.35 mm
W_2	Width of bottom feedline	0.33 mm
t	Length of tuning stub	3.07 mm
ε_{r1}	Relative permittivity of top substrate	2.2
ε_{r2}	Relative permittivity of bottom substrate	2.2

polarized element operating at Ku-band is presented to be used in panelized array for the earth terminals based on hybrid electronic/mechanical steering system in which the beam is electronically scanned in elevation by Rotman lens while the azimuthal movement is realized mechanically by rotating antenna panel. The radiating element is based on a concept presented in [8, 9] and the multibeam forming networks in [10, 11]. In consideration of the specifically operating frequency of Ku-band to design an antenna, the uplink (14–14.5 GHz) and downlink (12.25–12.75 GHz) frequency assigned to China for fixed satellite service (FSS) and broadcasting satellite service (BSS) are pragmatic.

2. Antenna Subarray

2.1. Radiating Element. Figure 1 shows the proposed dual-band dual-polarized rectangular patch antenna fed by coplanar microstrip line feed and slot-coupled feed. The antenna element is comprised of two dielectric layers with a common metal ground plane. The H-polarized feedline over the transmit frequency band of 14–14.5 GHz is printed onto the top side of a thick layer, while the V-polarized feedline over the receiving frequency band of 12.25–12.75 GHz is printed onto the bottom side of a thin layer. The rectangular radiating patch has the dimension of $L \times W$ with two same small slots, which make port 1 impedance matchable, on both sides of the coplanar microstrip line at the joint of patch and feedline. Port 2 is the slot-coupled feed with an H-shaped coupling slot cut in the ground plane and left below the radiating patch. The center arm and two side arms of the H-shaped coupling slot are of dimensions $S_{W1} \times S_{L1}$ and $S_{W2} \times S_{L2}$, respectively. With the utility of the H-shaped coupling slot instead of the conventional narrow slot, more degrees of freedom are provided to adjust the operating frequency of V-polarization on the condition that the size of radiating patch is decided in advance by operating frequency of H-polarization. The polarization values of the radiation generated from the two ports are orthogonal and linear, with low cross-polarization. These two feeding structures printed on different sides of the substrate simultaneously improve the isolation between the two feeding ports. Differing from the broadband feeding structure, the demand of 500 MHz bandwidth (less than 4%) for each polarization operating at respective band simplifies the feeding structure.

From Figure 1, it should be noted that the antenna element design is an optimization problem with multiparameters. The object function for impedance matching in the design is written as follows:

$$f_{\text{obj}} = \left|S_{11} - S_{\text{goal}}\,(\text{dB})\right|\Big|_{f(\text{GHz})\in[14.0,14.5]} + \left|S_{22} - S_{\text{goal}}\,(\text{dB})\right|\Big|_{f(\text{GHz})\in[12.25,12.75]}, \quad (1)$$

where S_{goal} is the expected value of isolation. The parameters to be optimized include all the variables of the element shown in Figure 1 except the thickness and permittivity of the two substrates. The input impedance of the two ports should be about 100 ohms to match the 50-ohm transmission line conveniently when arraying antenna elements. Taking genetic algorithm (GA) as the optimization algorithm MWS calculates S_{11} and S_{22} with several sets of parameters values in respective operating band. Then, the corresponding values of the object function f_{obj} are evaluated and new sets of parameters values are generated by GA before moving to the next iteration. The final parameters of the element meeting all the requirements of object function are listed in Table 1.

The performance of element is simulated and optimized by CST Microwave Studio. It can be seen observed from S-parameters shown in Figure 2 that good impedance matching is achieved at the dual band.

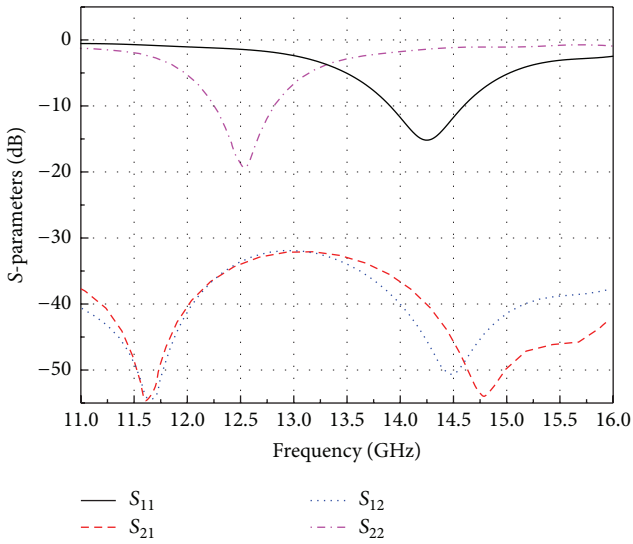

Figure 2: Simulated S-parameters for the dual-band dual-polarized antenna element.

2.2. Compact Feeding Networks. A feeding network is involved in designing impedance converter and power division. Two primary feeding techniques for dual-polarized linear arrays have been investigated in [8] by employing coplanar feeding networks and in [12] by applying slot coupling. In order to take full advantage of the limited element spacing, two compact feeding networks of a 1 × 8 linear array for each polarization are proposed as shown in Figure 3.

Naturally good isolation, achieved by placing the feeding networks for each polarization on respective side of the two layers of this antenna, makes it much easier to design the network of each polarization separately. A hybrid parallel/series feeding network is a trade-off between ideal radiation pattern obtained by parallel feeding providing good amplitude-phase consistency and bandwidth reduction by series feeding causing unevenness of amplitude and phase.

The 1 × 8 linear array shown in Figure 3 can be divided into two 1 × 4 subarrays, and only two elements are series-fed on each side of the subarray for both polarization cases. The first-row power dividers of each polarization are shown in Figure 3. All patches are matched by 130-ohm coplanar transmission lines for H-polarization feeding networks on the top and by 100-ohm coupling transmission lines for V-polarization on the bottom. Due to the limitation of element spacing decided by high operating frequency (14.25 GHz) (i.e., the interval between two elements is small for low operating frequency (12.5 GHz)), the concave transmission lines on the bottom are aimed at compensating the phase difference to feed in phase. The second-row power dividers are designed to connect two parallel 1 × 4 subarrays, shown in Figure 3. 180° phase difference should be compensated by bending the transmission line of the second row and offsetting the trunk line on the bottom for V-polarization since mirror symmetry of the two subarrays causes reverse phase. Two microstrip-to-coaxial structures are used at H-port and V-port to accommodate SMA, respectively.

Figure 4 shows that good performance is achieved for a 1 × 8 linear array operating at dual band with high isolation between the two input ports.

2.3. Construction and Validation of the 8 × 10 Array. The 8 × 10 antenna array as shown in Figure 5, fed by a multibeam feeding network (a 7 × 10 Rotman lens), is composed of ten duplicated 1 × 8 linear arrays with linear array spacing of 16 mm ($0.76\lambda_{TX}$ or $0.67\lambda_{RX}$). The performance of the 8 × 10 array is simulated and optimized by CST Microwave Studio.

As shown in Figures 6 and 7, benefitting by the simple but effective feeding networks, the cross-polarization is very low at dual band for each copolarization.

3. Rotman Lens Design

A multibeam antenna with adaptive beam switching is one of the capable antennas for scanning with wide angle coverage. Multibeam forming networks, such as Butler matrix and lens, are key technology for multibeam antennas. Due to the properties of simple design and compact size, Rotman lens became attractive in electronic scanning applications. The modified design procedures of Rotman lens and phase shifter network of substrate integrated waveguide (SIW) proposed in [11] are adopted in this paper to design a multibeam forming network. A hybrid microstrip/SIW Rotman lens as represented in Figure 8, of which the main body is manufactured by microstrip transmission lines and phase shifter network by SIW, is designed to operate in the 12.1–14.8 GHz band and realized on a microwave substrate with a relative permittivity of 2.2 and a thickness of 1.5 mm. This hybrid structure combines the properties of flexible layout of microstrip transmission lines and low loss of SIW. The lens can generate 7 beams for 10 linear arrays with coverage of −30°~30° to implement scanning by switching. The 10 dummy ports, which are terminated with 50-ohm chip resistors as matched absorbing loads, are used to realize sidelobe suppression.

CST simulations in the 11–15 GHz band were employed to predict the scattering parameters for Rotman lens. Figures 9 and 10 depict the simulated amplitude and phase distribution from input port 1 and port 4 to output ports at 12.25, 12.5, 12.75, 14.0, 14.25, and 14.5 GHz, respectively. It can be seen that the amplitude distribution is reasonably rippled within 4 dB and phase distribution is almost linear. Rotman lens is designed to offer 7 different sets of equal relative phase differences with acceptable errors corresponding to 7 beam ports to form 7 different pointing beams when exciting array composed of 10 linear subarrays.

4. Simulation of Complete Array

In order to analyze the performance of the multibeam forming network, that is, the Rotman lens designed in Section 3, the simulated values of amplitude and phase distributions

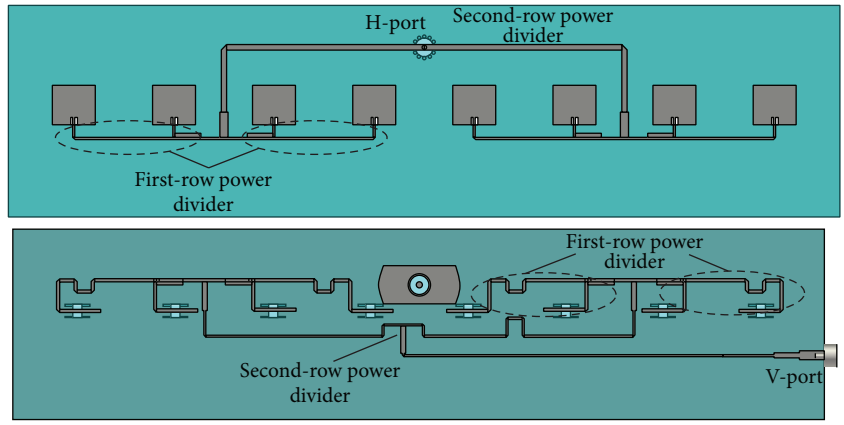

Figure 3: The layout of the 1 × 8 array using the compact feeding networks.

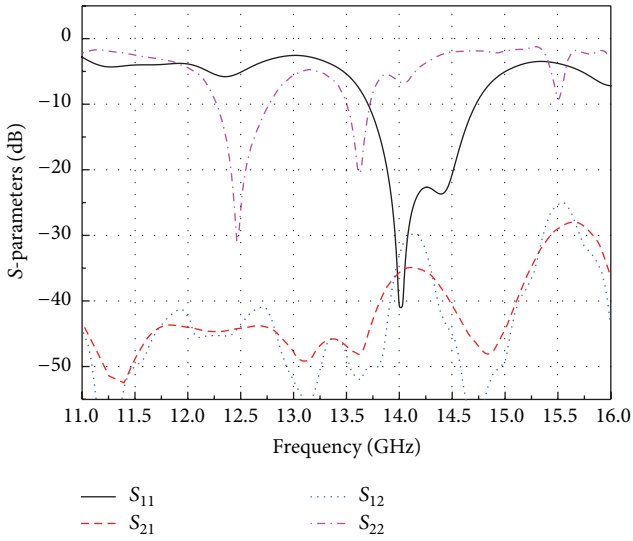

Figure 4: Simulated S-parameters for the 1 × 8 linear array.

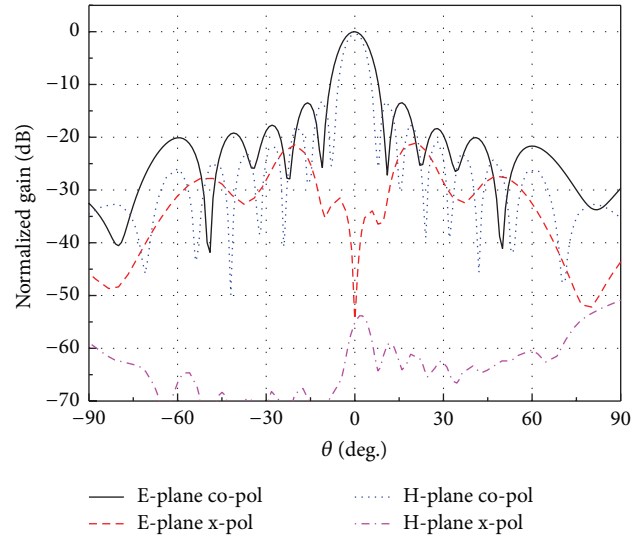

Figure 6: Simulated radiation patterns for V-port of the 8 × 10 array at 12.5 GHz.

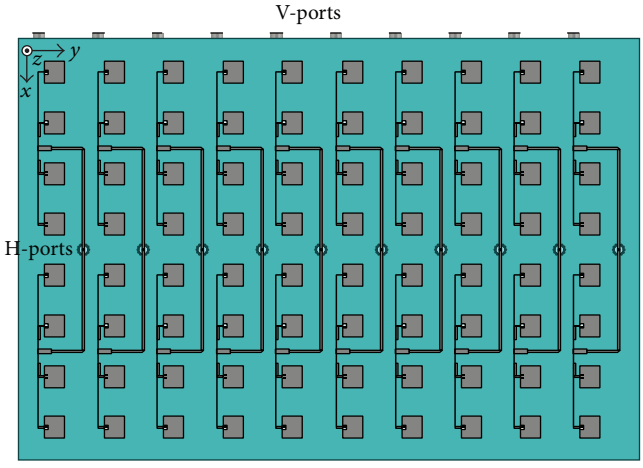

Figure 5: 8 × 10 dual-polarized Ku-band microstrip patch antenna array simulation model.

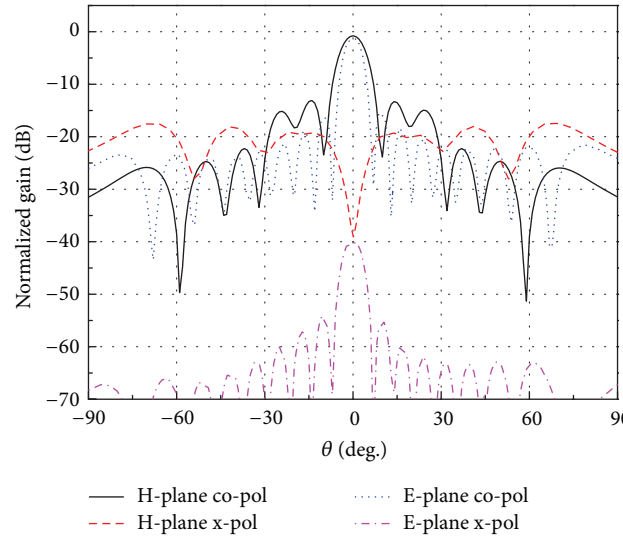

Figure 7: Simulated radiation patterns for H-port of the 8 × 10 array at 14.25 GHz.

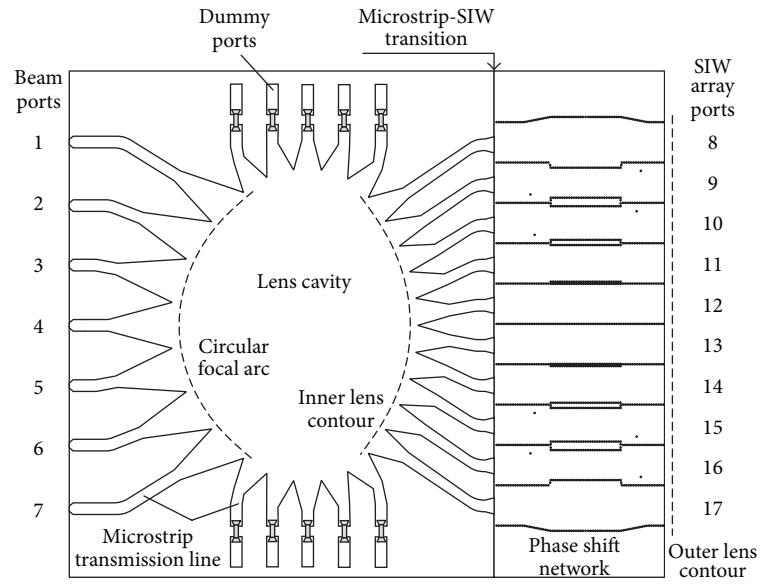

Figure 8: Geometry of the Rotman lens.

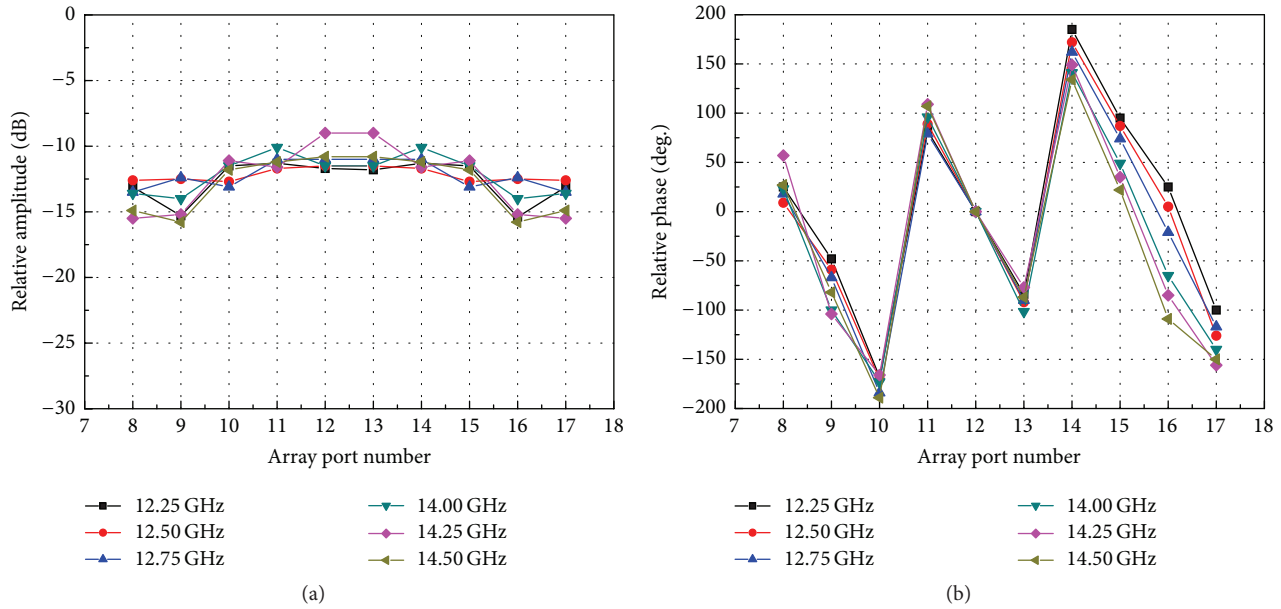

Figure 9: (a) Array ports relative amplitude distribution excited by edge port 1. (b) Array ports relative phase distribution excited by edge port 1.

obtained by exciting 7 beam ports are substituted as exciting source of the 8 × 10 antenna array for both polarization values.

The simulated E-plane beam patterns for H-polarization are shown in Figure 12. It can be seen that the 5 dB beam widths are approximately 10°, 10°, 11°, and 12° corresponding to input ports 1–4, respectively, and the corresponding beam directions point to 27°, 17°, 9°, and 0°, respectively. The gains for each port are 20.9, 22, 22.8, and 23.5 dBi corresponding to ports 1–4, respectively. The simulated H-plane beam patterns for V-polarization are shown in Figure 11. It can be seen that the 5 dB beam widths are approximately 10°, 11°, 12°, and 12° corresponding to input ports 1–4, respectively, and the corresponding beam directions point to 26°, 17°, 9°, and 0°, respectively. The gains for each port are 19.8, 21, 22.1, and 22.5 dBi corresponding to ports 1–4, respectively.

In Figure 13, a schematic overview of the dual-polarized antenna TX/RX system architecture is presented to achieve one-dimensionally electronic scanning in a shared aperture.

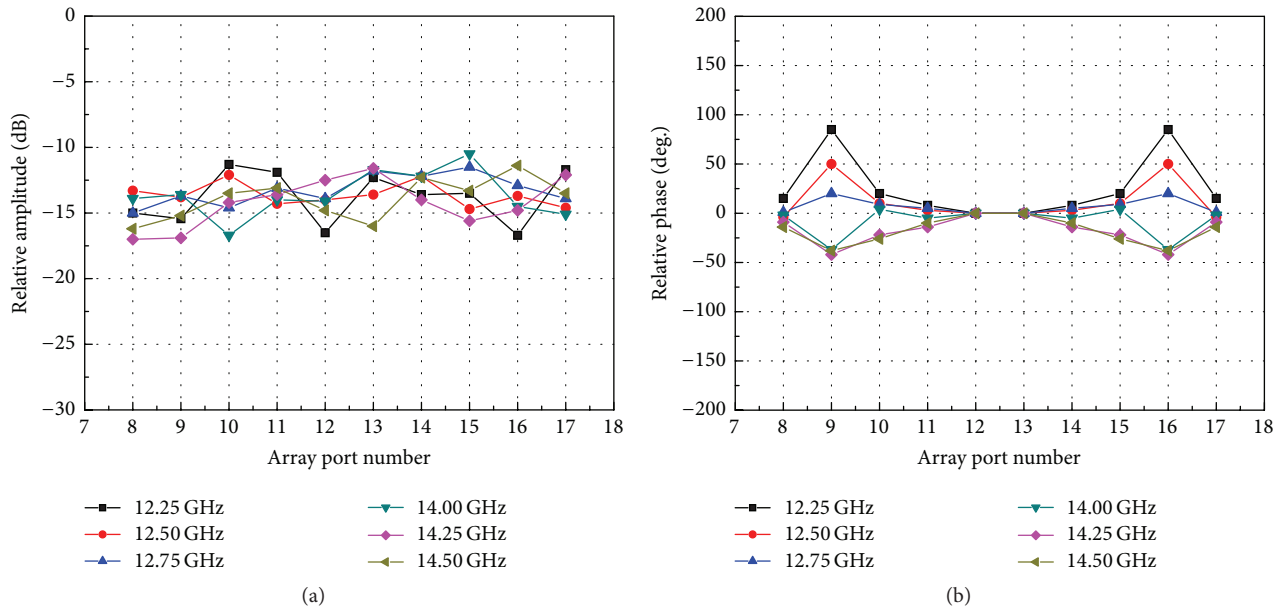

FIGURE 10: (a) Array ports relative amplitude distribution excited by center port 4. (b) Array ports relative phase distribution excited by center port 4.

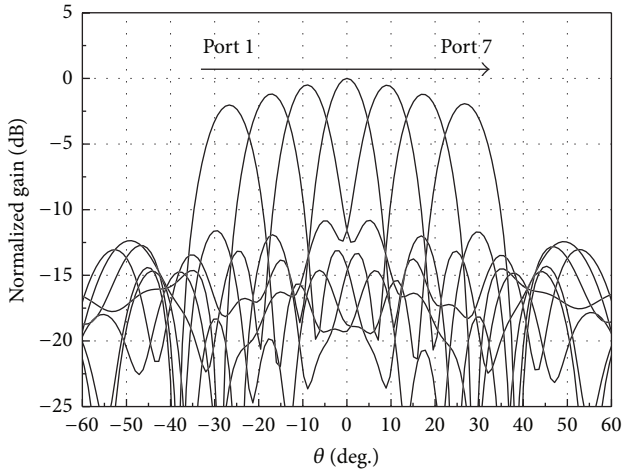

FIGURE 11: Radiation patterns of antenna array excited by amplitude and phase distributions of the Rotman lens at 14.25 GHz for H-polarization.

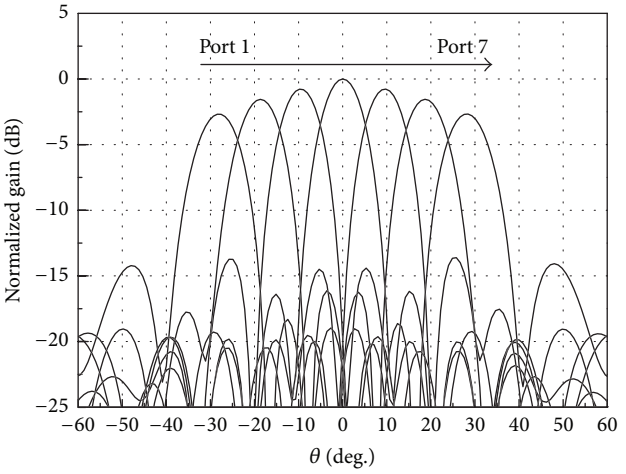

FIGURE 12: Radiation patterns of antenna array excited by amplitude and phase distributions of the Rotman lens at 12.5 GHz for V-polarization.

In order to realize 2D scanning, we can mount the antenna panel on a mechanical rotation table as depicted in Figure 14. Furthermore, low elevation angle will be covered by tilting the antenna panel with a higher profile.

5. Conclusion

In this paper, a multibeam dual-band orthogonal linearly polarized antenna array has been presented. Two feeding techniques have been used on each side of the substrate to increase the isolation between transmitting and receiving band and improve the cross-polarization between the two polarization values. The planar antenna array can be mounted on an azimuthally rotatable servo platform to realize hybrid electronic/mechanical scanning and further to automatically track communication satellites. More subarrays could be assembled to obtain higher gain. The simulated results show that the performance of the antenna array has a potential capacity to be a new option for Multimedia Satellite mobile communication.

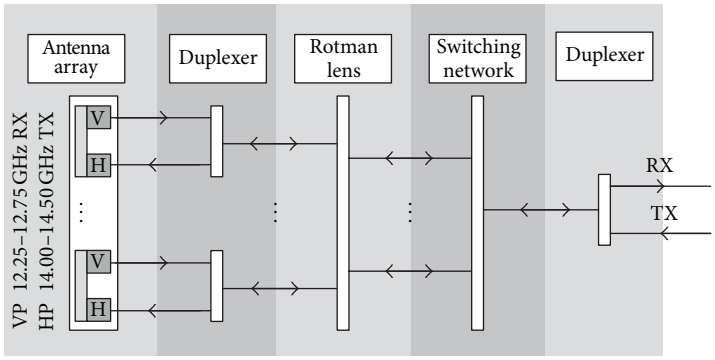

Figure 13: Schematic overview of a Ku-band transmit-receive array.

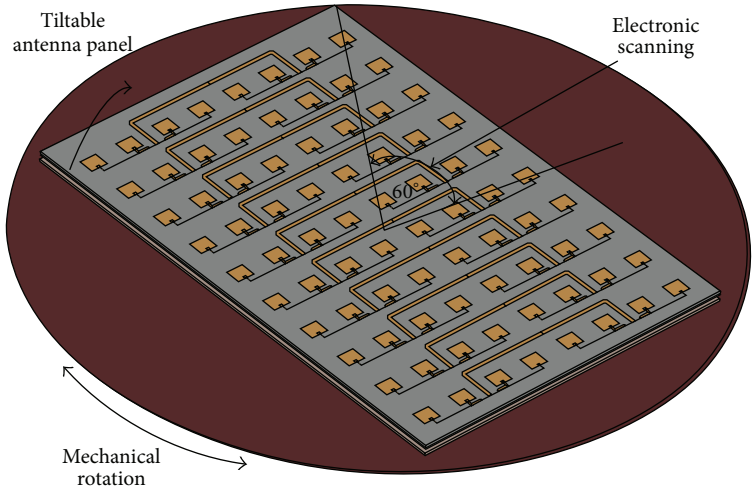

Figure 14: Sketch of the hybrid scanning array structure.

Conflict of Interests

The authors declare that there is no conflict of interests regarding the publication of this paper.

Acknowledgment

This work is sponsored by the National Nature Science Foundation of China under Grant no. 61171016.

References

[1] J. Thornton, A. White, and G. Long, "Multi-beam scanning lens antenna for satellite communications to trains," *Microwave Journal*, vol. 52, no. 8, pp. 56–70, 2009.

[2] L. Marcellini, R. Lo Forti, G. Bellaveglia, A. Colasante, F. Maggio, and O. Russo, "Multi-reflector multi-band antennas for airborne and maritime broadband applications," in *Proceedings of the 3rd IEEE-APS Topical Conference on Antennas and Propagation in Wireless Communications (APWC '13)*, pp. 1131–1134, IEEE, Torino, Italy, September 2013.

[3] L. Baggen and S. Holzwarth, "Satcom-on-the-move: digital beam forming versus phased array," in *Proceedings of the 8th European Conference on Antennas and Propagation (EuCAP '14)*, pp. 2610–2614, The Hague, The Netherlands, April 2014.

[4] M. Shelley and J. Vazquez, "Low profile scanning antennas for satcom 'on-the-move'," in *Proceedings of the European Workshop on Mobile/Personal Satcoms and Advanced Satellite Mobile Systems Conference*, pp. 1–6, 2004.

[5] S. Vaccaro, F. Tiezzi, M. F. Rúa, and C. D. G. De Oro, "Ku-band low-profile Rx-only and Tx-Rx antennas for mobile satellite communications," in *Proceedings of the 4th IEEE International Symposium on Phased Array Systems and Technology (ARRAY '10)*, pp. 536–542, IEEE, Waltham, Mass, USA, October 2010.

[6] S. Vaccaro, F. Tiezzi, D. Llorens, M. F. Rúa, and C. D. G. De Oro, "Ku-band low profile antennas for mobile satcom," in *Proceedings of the 4th Advanced Satellite Mobile Systems (ASMS '08)*, pp. 24–28, Bologna, Italy, August 2008.

[7] W. Rotman and R. F. Turner, "Wide-angle microwave lens for line source applications," *IEEE Transactions on Antennas and Propagation*, vol. 11, no. 6, pp. 623–632, 1963.

[8] N. Jin and Y. Rahmat-Samii, "Microwave holographic tuning of a dual-polarized Ku-band microstrip antenna array," in *Proceedings of the 2nd European Conference on Antennas and Propagation (EuCAP '07)*, pp. 1–5, IET, Edinburgh, Scotland, November 2007.

[9] Z. Chen, Z. Zhang, J. Yin et al., "Dual-polarized multi-layer microstrip array antenna with H-shaped coupling slot," in *Proceedings of the International Conference on Microwave*

and Millimeter Wave Technology (ICMMT '12), pp. 1–3, IEEE, Shenzhen, China, May 2012.

[10] S. Christie, R. Cahill, N. B. Buchanan et al., "Rotman lens-based retrodirective array," *IEEE Transactions on Antennas and Propagation*, vol. 60, no. 3, pp. 1343–1351, 2012.

[11] Y. J. Cheng, W. Hong, K. Wu et al., "Substrate integrated waveguide (SIW) Rotman lens and its Ka-band multibeam array antenna applications," *IEEE Transactions on Antennas and Propagation*, vol. 56, no. 8, pp. 2504–2513, 2008.

[12] A. Vallecchi and G. B. Gentili, "Design of dual-polarized series-fed microstrip arrays with low losses and high polarization purity," *IEEE Transactions on Antennas and Propagation*, vol. 53, no. 5, pp. 1791–1798, 2005.